Theoretical Characterization of the Vibrational Properties at the Aluminum/*trans*-Polyacetylene Interface

V. Parente,[†,‡] C. Fredriksson,[‡] A. Selmani,[‡] R. Lazzaroni,[†,§] and J. L. Brédas*[,†]

Centre de Recherche en Electronique et Photonique Moléculaires, Service de Chimie des Matériaux Nouveaux, Université de Mons-Hainaut, B-7000 Mons, Belgium, and Centre de Recherche Appliquée sur les Polymères (CRASP), Département de Génie Chimique, Ecole Polytechnique de Montréal, P.O. Box 6079, Station Centre-Ville, Montréal, Québec H3C 3A7, Canada

Received: November 21, 1996; In Final Form: February 5, 1997[⊗]

We investigate theoretically the geometric structure and vibrational properties of complexes of polyenes with aluminum atoms that constitute model systems for the species formed at the interface between aluminum and polyacetylene. The calculations are performed with two quantum-mechanical techniques: *ab initio* Hartree−Fock and density functional theory in the local spin density approximation. These methods are first applied to a polyene molecule, all-trans octatetraene, and the calculated vibrational spectra are compared to existing experimental and theoretical data. The molecule is then made to interact with two aluminum atoms in various configurations. Since the metal atoms form covalent bonds with carbon atoms in the central part of octatetraene, strong geometric modifications occur along the conjugated system, which in turn deeply affect the vibrational spectra. These results allow us to derive the expected infrared signature of the chemical species present at the interface.

1. Introduction

Aluminum has turned out to be one of the most interesting low-workfunction metals for use as electron-injecting contact in electronic devices based on organic semiconductors.[1] Although metals such as calcium have a lower workfunction, and thereby provide a more efficient electron injection than aluminum,[2] the relatively stable character of the Al/organic semiconductor interface makes this metal very attractive for applications. One of the reasons for this stability is the covalent bonding between Al and the polymer chains at such interfaces,[3] which provides better conditions for contact formation than calcium, since in the latter case bonding is ionic in character and the metal atoms diffuse more easily into the organic material.[4]

Over the past few years, photoelectron spectroscopy measurements have been performed to study the interface formation between aluminum and organic semiconductors.[3,5] The evolution of the electronic structure of the semiconductor at the surface was monitored during vapor deposition of aluminum monolayers. To interpret such photoelectron spectra, several theoretical studies have been performed at the quantum-chemical level.[6−11] These studies consistently predict the formation of covalent Al−C bonds and indicate that significant modifications occur to the upper π-electron band of the organic systems. These results are in full agreement with existing experimental data.

Theoretical studies performed at the *ab initio* Hartree−Fock (HF) level of calculation on Al/polythiophene,[6] Al/polyene,[7] and Al/poly(*p*-phenylenevinylene) (Al/PPV)[8] complexes show that Al binds to a carbon atom of a π-conjugated system by a single Al−C bond. In the case of polythiophene, the preferred reaction sites are the α-carbons (relative to sulfur) of the thiophene rings, and in the case of PPV, reactions with the vinylene moieties are the most favorable. Upon bond formation, the carbon atoms involved in the metal bonding rehybridize, from sp^2 in the pristine polymer segment to sp^3. Investigations performed at the density functional theory (DFT) level within the local spin density approximation (LSDA) show a slightly different picture. According to LSDA results on Al/polyene[9] and Al/benzene complexes,[10] the Al atoms bind with multiple covalent bonds to carbon sites on the π-conjugated system. A similar bonding mechanism to multiple carbon sites is found in LSDA calculations on Al/(oligo)thiophene clusters.[11] Both the HF and LSDA quantum-mechanical methods have their shortcomings: the HF method, by definition, neglects electron correlation, while the LSDA method, which takes correlation energy explicitly into account, is known to produce overbinding.[12] We note that post Hartree−Fock Møller−Plesset perturbation theory (MP2) calculations indicate the important role of correlation in the evaluation of vibrational frequencies,[13−15] such as those investigated in this work.

In this study, we have performed a theoretical analysis of the vibrational properties of Al/polyene complexes, comparing the results of HF and LSDA methods. The evolution of the vibrational normal modes upon Al bonding, as obtained from the two computational techniques, is used to derive characteristics that, ultimately combined with surface-sensitive vibrational measurements performed during metallization, could provide useful additional information concerning the chemical structure in the initial stages of interface formation.

2. Methodology

The results presented here are based on Hartree−Fock (HF) and local spin density approximation (LSDA) calculations performed using the Gaussian 92/DFT and Gaussian 94 quantum-chemistry codes.[16] Full geometry optimizations are carried out in order to obtain the ground-state chemical structures. The 6-31G* basis set[17] is used for the study of the Al/polyene complexes. Tests were performed on butadiene to compare the results obtained with the 6-31G* and 6-31G** basis sets as well as other split valence (augmented with polarization functions) Gaussian basis sets of similar quality that have been

[†] Université de Mons-Hainaut.
[‡] Ecole Polytechnique de Montréal.
[§] Chercheur qualifié du Fonds National Belge de la Recherche Scientifique (FNRS).
[⊗] Abstract published in *Advance ACS Abstracts,* May, 1, 1997.

S1089-5647(96)03881-3 CCC: $14.00

TABLE 1: Structural Data (in Å) for *trans*-Butadiene As Calculated by Various Quantum-Mechanical Techniques and As Derived from Experiment (See Text for Notations)

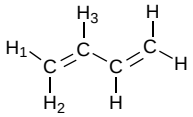

	this work					literature				
	LSDA[a]	LSDA[b]		HF[b]		HF [21]	MP2[13]	MP2[13]		
	DNP	DZVP	6-31G**	DZVP	6-31G**	6-31G*	6-31G*	6-311G(2d,p)	expt[21]	expt[13]
C═C	1.338	1.344	1.340	1.326	1.322	1.323	1.343	1.339	1.341	1.342−1.349
C−C	1.435	1.443	1.438	1.468	1.467	1.468	1.456	1.454	1.463	1.463−1.467
C−H_1	1.096	1.094	1.093	1.074	1.075	1.075	1.084	1.083	1.090	1.093−1.108
C−H_2	1.099	1.096	1.096	1.075	1.077	1.077	1.086	1.085	1.090	1.093−1.108
C−H_3	1.101	1.100	1.100	1.076	1.079	1.078	1.090	1.088	1.090	1.093−1.108

[a] DMol package. [b] Gaussian 92/DFT.

specifically optimized for density functional purposes (DZVP, double zeta valence polarized). As detailed in the following section, the 6-31G* basis set provides adequate chemical structures and vibrational normal modes within both the HF and LSDA methods. We have observed that polarization functions on the hydrogen atoms do not affect the calculated vibrational spectra considerably. This observation is consistent with the work of Lee *et al.*[13,14] A comparison was also made with results from the DMol DFT package[18] utilizing a high-quality numerical basis set (DNP, double-numeric plus polarization), in order to verify that the LSDA method itself is consistent. The Vosko−Wilk−Nusair expression[19] for the local correlation potential combined with the Slater local exchange functional is used in the LSDA-based calculations.

A second series of tests have also been performed on the octatetraene molecule, in order to determine the effect that the use of nonlocal functionals (used during the SCF procedure) in the DFT formalism might have on both molecular geometry and vibrational frequencies. The nonlocal functionals we considered are the Becke 88[20] gradient-corrected exchange potential associated with either the Lee−Yang−Parr,[21] Perdew 86,[22] or the Perdew−Wang 91[23] gradient-corrected correlation potentials. Those DFT calculations have been performed using the 6-31G* basis set mentioned above (the nonlocal functionals are referenced in the text as BLYP, BP86, and BPW91, respectively).

The vibrational normal modes are calculated according to Wilson's method,[24] by diagonalizing the force constant matrix at the fully optimized geometry. It is well-known that the force constants generated by HF-based calculations are considerably overestimated. This results in a displacement of the calculated vibrational normal modes toward higher frequencies, compared to experiment. To overcome this problem, it is necessary to rescale the force constants by a factor that generally depends on the vibrational mode considered;[13−15] in this way, the calculated spectrum is fitted to the corresponding experimental data. Since the scope of this study is not to match the HF results quantitatively with experiment, but rather to observe the characteristic trends in modifications of the vibrational properties upon aluminum metallization, we have corrected for the shortcomings of the HF method simply by contracting the final spectrum by 89%; this approach has been used in previous studies of similar systems to generate vibrational spectra.[25] The LSDA method, in contrast, inherently produces more accurate force constants and, therefore, usually gives frequencies matching experimental spectra without scaling. The infrared intensities are calculated on the basis of the squares of the derivatives of the molecular dipole moments with respect to the atomic coordinates. However, since *ab initio* intensities frequently differ by ±20−50% compared to experimental data,[26] they can only serve as rough estimates.

We have chosen to perform the calculations on the *trans*-octatetraene molecule (C_8H_{10}), representing a segment of *trans*-polyacetylene. The length of the polyene is chosen so as to prevent the hydrogen terminated ends of the polyene from interfering significantly with the central Al−C bonds. The starting geometries of the Al/polyene complexes used to model the interactions are based on chemical structures derived from previous studies using the *ab initio* HF and LSDA methods, respectively.[7,9,27] By including two aluminum atoms in the complexes, we only consider closed-shell systems, thereby ensuring that the complexes are described well at the restricted HF level. The situations where the Al atoms are placed on opposite sides of the polyene plane and on the same side are both considered. As presented in the discussion, the HF and LSDA optimized geometries lead to the same basic conclusions. However, the conformations present some differences. To better understand those differences, each optimized geometry at both the HF and LSDA level has been used as the starting point of an MP2 geometry optimization.

The electron distribution has been analyzed by means of both Mulliken population analysis[28] and natural population analysis, NPA (based on the natural bond orbital analysis, NBO).[29]

3. Results and Discussion

Pristine Butadiene and Octatetraene. To check the validity of our theoretical approach, we first considered the butadiene and octatetraene molecules. These molecules have been thoroughly studied, theoretically as well as experimentally,[13−15,25,31−32] and serve as relevant model compounds for π-conjugated polymers. The most important structural properties in the context of our work are the carbon−carbon bond lengths since these are related to the degree of conjugation within the molecule and may switch (double/single) character upon aluminum bonding.

The results obtained on butadiene are presented in Table 1. The geometrical features are found to be generally well described by all the theoretical methods included in the comparison. The differences between the HF and LSDA structural data, such as the degree of carbon−carbon bond length alternation, have been discussed in previous studies of comparable π-conjugated systems.[9,27] The tendency for LSDA-based methods to slightly underestimate C−C bond lengths and for uncorrelated HF techniques to slightly underestimate C═C and C−H bond lengths is confirmed in the present calculations. Although we have chosen not to include the bond angles in the table, these are also found to be well described by these

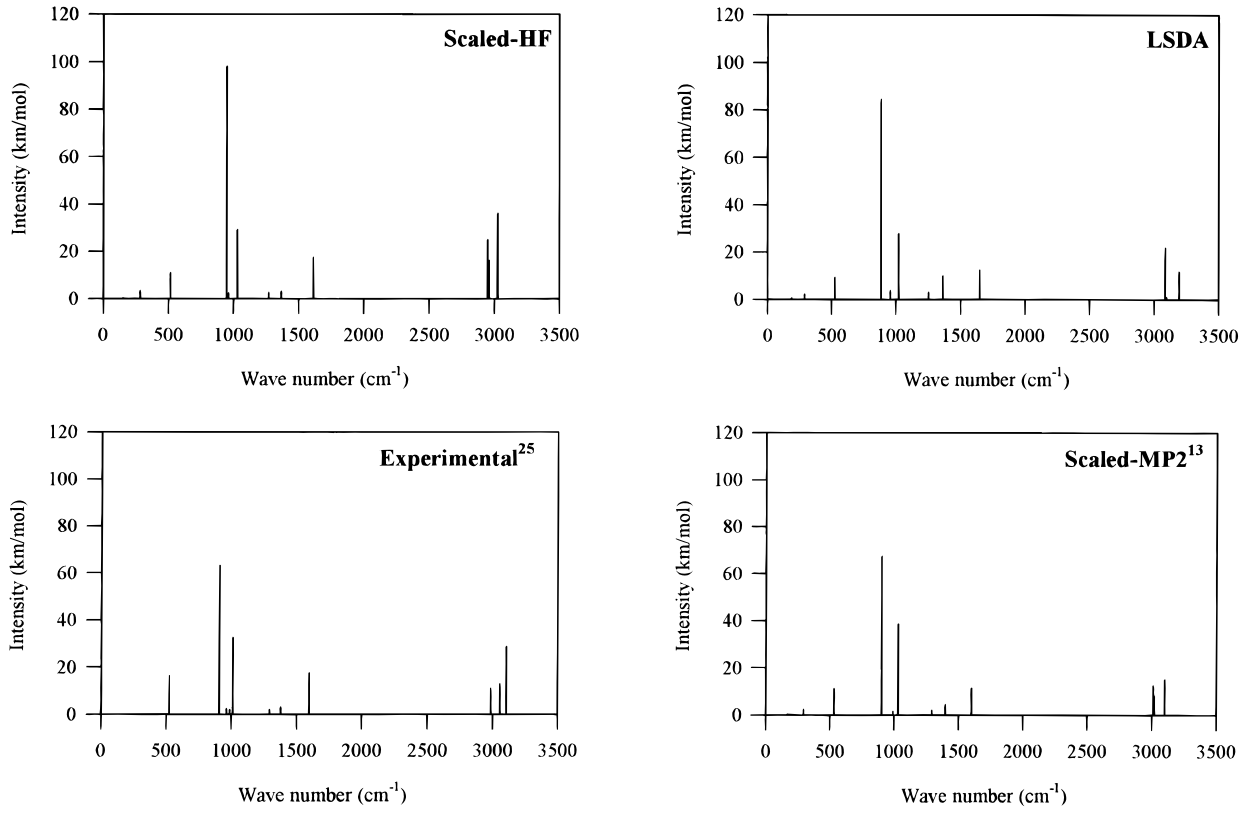

Figure 1. Infrared spectra of butadiene: (top left) scaled HF calculation; (top right) LSDA calculation; (bottom left) experiment;[25] (bottom right) scaled MP2 calculation.[13]

theoretical methods. We conclude from these data that the results obtained at the HF and LSDA level are very similar whatever the basis set, *i.e.*, a Pople basis set optimized for HF calculations or a Gaussian basis set optimized for DFT calculations.

Both theoretical approaches also accurately reproduce the vibrational spectra for butadiene. The experimental IR[25] spectra and calculated vibrational spectrum are shown in Figure 1, and the values of the frequencies with their symmetry assignment are given in Table 2. The agreement between the calculated LSDA and scaled HF frequencies with the MP2 results of Lee *et al.*[13] and experimental data[13,25] is good. Except for the first normal mode, all frequencies are within 4% of the experimental values. The existing 20−50 cm^{-1} discrepancies could be due to the differences observed in the geometry of the butadiene molecule, where underestimation of C−C or overestimation of C═C bond lengths occurs, depending on the technique. Moreover, the use of the same scaling factor for all vibrational modes in the HF approach can also lead to slight discrepancies in the frequency values.

As can be seen clearly from Figure 1, the most active IR modes appear very similar in all spectra. These are (i) the out-of-plane cis and trans wagging modes, just above 500 and 1000 cm^{-1}, respectively; (ii) the strongest peak, which is an out-of-plane $=CH_2$ wagging mode below 1000 cm^{-1}; (iii) the asymmetric C═C stretching mode above 1600 cm^{-1}; and finally (iv) the optically active band of C−H stretches beginning around 3000 cm^{-1}. The main difference between the HF and LSDA calculated spectra arises essentially from the 3000 cm^{-1} band, where frequencies are slightly underestimated in HF spectra and overestimated in LSDA spectra. Note also a slight overestimation of the asymmetric $=CH_2$ scissor intensity at 1363 cm^{-1} in the LSDA spectrum. However, these differences are not significant enough to discriminate between the performances of the theoretical methods. The overall agreement, including the distribution of intensities, clearly shows that both theoretical methods at this level do give reliable descriptions of the vibrational properties of polyenes.

TABLE 2: Vibrational Frequencies (cm^{-1}) for *trans*-Butadiene and Their Symmetry Assignments (Theoretical Methods and Experimental Data); The IR Active Modes Are Those with A_u or B_u Symmetry

	this work		literature		
	LSDA 6-31G**	scaled HF 6-31G**	scaled MP2[13] 6-311G(2d,p)	expt[13−21]	sym
ν1	187	148	169	162, 163, 163, 164	A_u
ν2	288	284	295	300, 301, 301, 303	B_u
ν3	503	490	513	512, 512, 513, 513	A_g
ν4	527	517	533	525, 525, 525, 535	A_u
ν5	762	757	768	752, 753, 753, 754	B_g
ν6	885	852	895	887−888, 890, 892	A_g
ν7	889	949	902	905, 908, 908, 908	A_u
ν8	893	950	902	908, 908, 910, 911	B_g
ν9	956	964	972	965, 966, 967, 974	B_g
ν10	958	991	991	985, 987, 988, 990	B_u
ν11	1021	1030	1032	1013, 1013, 1014, 1022	A_u
ν12	1207	1175	1209	1203, 1203, 1205, 1206	A_g
ν13	1253	1271	1290	1277, 1278, 1279, 1291	A_g
ν14	1265	1273	1291	1282, 1294, 1294, 1296	B_u
ν15	1363	1367	1395	1380, 1381, 1381, 1384	B_u
ν16	1418	1426	1458	1438, 1441, 1441, 1442	A_g
ν17	1647	1616	1602	1596, 1597, 1597, 1598	B_u
ν18	1704	1686	1659	1638, 1643, 1644, 1644	A_g
ν19	3077	2942	3010	2982, 2984, 2985, 2986	B_u
ν20	3086	2947	3006	3008, 3013, 3014, 3014	A_g
ν21	3096	2957	3016	3013, 3014, 3025, 3028	A_g
ν22	3097	2958	3019	3055, 3056, 3056, 3062	B_u
ν23	3194	3023	3102	3095, 3101, 3102, 3103	B_u
ν24	3194	3023	3102	3100, 3101, 3102, 3105	A_g

The octatetraene molecular geometries obtained at various theoretical levels are presented in Table 3. As for the butadiene molecule, the LSDA C═C bond lengths are very close to those obtained at the MP2 level, while the C−C bond lengths are underestimated. When using nonlocal functionals, this tendency

TABLE 3: Structural Data (in Å) for *trans*-Octatetraene As Calculated by Various Quantum-Mechanical Techniques and As Derived from Experiment (See Text For Notations); A 6-31G* Basis Set Has Been Used for All the Results Presented in This Table

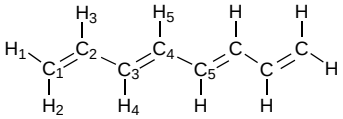

	this work					literature	
	HF	LSDA	BLYP	BP86	BPW91	MP2[15]	expt[14]
C_1═C_2	1.324	1.345	1.357	1.356	1.356	1.347	1.336
C_2−C_3	1.463	1.428	1.450	1.447	1.446	1.449	1.451
C_3═C_4	1.331	1.357	1.371	1.370	1.369	1.357	1.327
C_4−C_5	1.459	1.420	1.442	1.439	1.438	1.443	1.451
C_1−H_1	1.075	1.094	1.093	1.094	1.092	1.085	
C_1−H_2	1.077	1.097	1.095	1.097	1.095	1.087	
C_2−H_3	1.078	1.101	1.098	1.100	1.098	1.090	
C_3−H_4	1.079	1.101	1.098	1.100	1.098	1.092	
C_4−H_5	1.079	1.102	1.099	1.101	1.098	1.092	

is reversed: C−C single bond lengths become very close to the experimental and MP2 values, while double bonds are slightly overestimated. Note that the experimental data have been reported with a possible experimental error as large as 0.02 Å (see refs 14 and 15 for further details). The effect of gradient-corrected functionals on the C−H bond lengths is not as significant.

The calculated vibrational frequencies of the octatetraene molecule, obtained at the various theoretical levels, are given in Table 4, where they are compared to recent MP2/6-31G* and experimental results.[15] From Table 4, it appears that the vibrational frequencies calculated in this work are in overall good agreement with the published results. As it is the case for the butadiene molecule, small discrepancies appear, especially for the modes located around 1600 cm^{-1}. It is has been shown that the frequencies of those vibrational modes, involving the carbon−carbon stretching, are overestimated at the HF/6-31G* level and that inclusion of electron correlation via the MP2 approach leads to results in closer agreement with experiment. Moreover, in a work on *trans*-octatetraene, Lee *et al.*[14] have reported that higher frequencies tend to be overestimated while the lower frequencies do not, application of an exponential scaling being therefore more suitable than uniform scaling. In the DFT results, the same modes (around 1600 cm^{-1}) are also overestimated.

When comparing the results obtained at the local level with those obtained with nonlocal functionals, it appears that the latter do not have a strong influence on the vibrational frequencies (except for the modes above 1600 cm^{-1}, which remain overestimated but are better described). The relative IR intensities are also well reproduced at both levels. Following those observations, together with those relative to the octatetraene geometry, the use of nonlocal functionals is not essential, but is more time consuming; as a result, the calculations on the aluminum complexes are performed at the LSDA level. The theoretical vibrational spectra of the octatetraene molecule, obtained with both HF and LSDA techniques, are presented in Figure 2, for the sake of comparison with the vibrational spectra of the complexes of octatetraene with aluminum.

From Figure 2, it is clear that the overall vibrational characteristics for the octatetraene molecule are, not unexpectedly, very similar for the two computational methods, and analogous to butadiene. The strongest intensities in the theoretical spectra correspond to the peak located just above 1000 cm^{-1}, *i.e.*, the out-of-plane trans wagging mode (the hydrogen atoms moving perpendicularly to the backbone plane while the carbon atoms move in the opposite direction). A second peak with a strong intensity is also observed in both spectra (946 cm^{-1} in HF and 876 cm^{-1} in LSDA); this peak is related to the out-of-plane wagging of CH_2 terminal groups and constitutes the most intense mode in the butadiene spectra. Both spectra are also similar in the following regions: (i) three skeletal modes in the region between 400 and 600 cm^{-1}; (ii) the bending modes of the C−H bonds in the region between 1100 and 1300 cm^{-1}; (iii) the carbon−carbon stretching modes at 1597 and 1679 cm^{-1} in the HF calculations and at 1614 and 1694 cm^{-1} in LSDA calculations; (iv) the intense C−H stretch around 3000 cm^{-1}, characterized by two strong bands in the HF spectrum and one in the LSDA spectrum.

C_8H_{10}/Al_2 Complexes. We now focus our attention on the evolution of the chemical, structural, and vibrational properties upon Al bonding. We first discuss the chemical structure. The HF results on two possible configurations for Al bonding on octatetraene are shown in Figure 3.

Geometric Properties. The chemical structures of similar complexes have been previously investigated with semiempirical and *ab initio* HF methods; the results[7,9] show that each Al atom binds to a carbon atom by a single covalent Al−C bond that has a significant polar character. The present results confirm this behavior. No Al−Al bonding is predicted by *ab initio* HF methods even in the case where the Al atoms are located on the same side of the polyene plane. We observe that the Al bonding leads to a strong tendency for the bonded carbon sites to sp^3 hybridize, which tends to interrupt the π-conjugation along the carbon backbone; this causes some loss of planarity of the system (∼25°), which in turn is expected to impair the electronic transport properties. The HF results indicate that the Al−C bond is 2.06 Å, in agreement with the experimental estimate of 2.0 Å for a single Al−C bond in organoaluminum compounds.[33]

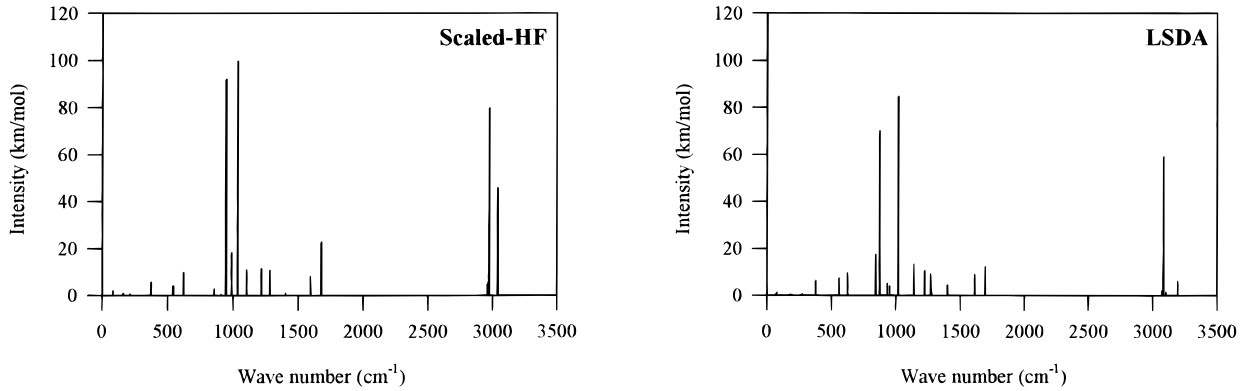

Figure 2. Calculated infrared spectra of pristine C_8H_{10}: (left) HF spectrum; (right) LSDA spectrum.

TABLE 4: Vibrational Frequencies (cm^{-1}) and Related Intensities (km/mol, between Parentheses) for Octatetraene, Calculated at the HF, LSDA, BLYP, BP86, and BPW91 Levels Using a 6-31G* Basis Set, Compared to Those Reported in the Literature[15] at the MP2/6-31G* Level and to Experimental Data (Experimental Intensities are Reported As Very Strong (vs), Strong (s), Medium (m), Weak (w), and Very Weak (vw); Modes with Zero IR Intensities Are the Raman Active Modes)

scaled HF	LSDA	BLYP	BP86	BPW91	scaled MP2[15]	expt[15]
55 (0.2)	66 (0.3)	62 (0.2)	62 (0.2)	62 (0.2)	60 (0.5)	
83 (2.0)	80 (1.1)	85 (1.1)	83 (1.1)	84 (1.1)	86 (1.1)	96 (vw)
134 (0.0)	163 (0.0)	159 (0.0)	157 (0.0)	157 (0.0)	149 (0.0)	
160 (0.8)	186 (0.4)	175 (0.3)	174 (0.4)	173 (0.4)	169 (0.3)	181 (vw)
213 (0.0)	213 (0.0)	219 (0.0)	215 (0.0)	216 (0.0)	222 (0.0)	
213 (0.5)	276 (0.6)	266 (0.3)	265 (0.5)	264 (0.5)	241 (0.7)	245 (w)
320 (0.0)	341 (0.0)	334 (0.0)	335 (0.0)	335 (0.0)	332 (0.0)	343
331 (0.0)	355 (0.0)	343 (0.0)	343 (0.0)	342 (0.0)	335 (0.0)	343 (vw)
373 (5.7)	380 (6.3)	383 (6.4)	377 (6.3)	378 (6.3)	390 (3.9)	390 (w)
516 (0.0)	522 (0.0)	530 (0.0)	524 (0.0)	526 (0.0)	543 (0.0)	538
542 (4.0)	561 (7.2)	560 (7.2)	557 (7.3)	558 (7.3)	566 (3.3)	565 (m)
622 (9.8)	628 (9.5)	626 (6.2)	622 (7.8)	623 (7.8)	621 (11.2)	629 (m)
664 (0.0)	662 (0.0)	659 (0.0)	656 (0.0)	658 (0.0)	652 (0.0)	
854 (2.7)	847 (17.5)	843 (6.5)	837 (6.5)	840 (5.9)	836 (0.7)	840 (w)
906 (0.8)	868 (0.0)	865 (0.1)	860 (0.0)	865 (0.1)	866 (0.0)	877
906 (0.0)	876 (70.0)	869 (64.3)	865 (74.5)	870 (75.7)	895 (81.8)	896
930 (0.0)	895 (0.0)	881 (0.0)	875 (0.0)	879 (0.0)	895 (0.0)	900 (vs)
944 (0.0)	911 (0.0)	922 (0.0)	912 (0.0)	917 (0.0)	929 (0.0)	
946 (92.0)	933 (5.0)	936 (1.1)	934 (2.1)	937 (2.2)	934 (0.3)	
959 (0.0)	944 (0.0)	956 (0.0)	951 (0.0)	955 (0.0)	958 (0.0)	956
988 (18.3)	955 (4.0)	966 (1.0)	958 (1.6)	962 (1.7)	962 (0.0)	960
1019 (0.0)	1000 (0.2)	1010 (0.0)	1003 (0.0)	1007 (0.0)	998 (0.0)	
1033 (99.7)	1022 (84.8)	1032 (65.3)	1025 (82.2)	1030 (83.9)	1018 (139.0)	1011 (vs)
1084 (0.0)	1141 (13.1)	1148 (14.5)	1144 (14.3)	1149 (14.7)	1122 (0.0)	1136
1109 (11.0)	1198 (0.0)	1158 (0.0)	1168 (0.0)	1171 (0.0)	1131 (9.9)	1139 (m)
1163 (0.0)	1202 (0.0)	1196 (0.0)	1197 (0.0)	1201 (0.0)	1186 (0.0)	1179
1217 (11.4)	1223 (10.5)	1242 (9.8)	1232 (10.6)	1239 (10.2)	1224 (6.0)	1229 (m)
1271 (0.0)	1255 (0.4)	1286 (0.0)	1277 (0.0)	1283 (0.0)	1278 (0.0)	1280 (m)
1280 (10.8)	1272 (9.1)	1292 (4.1)	1284 (4.8)	1290 (4.3)	1283 (4.9)	1281
1286 (0.0)	1277 (1.5)	1297 (0.0)	1288 (0.0)	1294 (0.0)	1293 (0.0)	1291
1299 (0.2)	1285 (0.0)	1309 (1.0)	1300 (1.1)	1307 (1.0)	1294(0.0)	1299
1302 (0.0)	1297 (0.0)	1315 (0.0)	1308 (0.0)	1315 (0.0)	1294 (0.8)	1303 (vw)
1405 (1.1)	1400 (4.5)	1423 (0.8)	1414 (1.1)	1421 (1.1)	1404 (1.4)	1405 (m)
1422 (0.0)	1425 (0.0)	1447 (0.0)	1438 (0.0)	1445 (0.0)	1425 (0.0)	1423
1597 (8.1)	1614 (8.8)	1576 (5.1)	1580 (6.5)	1585 (6.5)	1554 (6.0)	1558−1569 (m)
1641 (0.0)	1660 (0.0)	1607 (0.0)	1618 (0.0)	1622 (0.0)	1600 (0.0)	1613
1679 (22.7)	1671 (0.0)	1625 (0.0)	1631 (0.0)	1635 (0.0)	1616 (0.0)	1613
1684 (0.0)	1694 (12.3)	1642 (13.7)	1651 (14.0)	1656 (14.6)	1630 (14.6)	1632 (s)
2958 (0.0)	3069 (0.2)	3051 (0.0)	3055 (0.0)	3073 (0.0)	2987 (0.0)	
2960 (4.9)	3072 (2.1)	3052 (5.3)	3057 (5.2)	3075 (5.8)	2989 (0.8)	2967 (m)
2964 (5.3)	3075 (0.7)	3055 (0.0)	3059 (0.0)	3076 (0.0)	2992 (0.0)	
2964 (0.0)	3079 (11.8)	3057 (1.8)	3062 (0.3)	3079 (0.4)	2995 (29.4)	3009 (s)
2968 (0.0)	3084 (59.0)	3064 (0.0)	3068 (0.0)	3086 (0.0)	3004 (0.0)	
2971 (36.7)	3084 (1.3)	3069 (107.3)	3071 (104.6)	3088 (102.7)	3004 (53.9)	
2974 (0.0)	3102 (0.9)	3081 (9.9)	3084 (6.5)	3099 (8.7)	3017 (0.0)	
2975 (79.9)	3103 (1.3)	3082 (10.3)	3084 (9.6)	3100 (8.5)	3017 (10.8)	3030 (s)
3040 (0.7)	3195 (5.9)	3162 (18.3)	3170 (1.9)	3185 (15.4)	3105 (0.0)	
3040 (45.7)	3196 (6.0)	3163 (18.7)	3170 (29.4)	3186 (15.8)	3105 (23.3)	3091 (m)

The optimized chemical structures of the two aluminum/octatetraene complexes, as calculated with the LSDA method, are shown in Figure 4 (see Table 2 to compare with the pristine *trans*-octatetraene geometry). Upon bonding, Al atoms form multiple bonds with the carbon backbone, the shortest Al−C bond lengths being close to the 2.14 Å value found experimentally for a trimethyl aluminum dimer.[33] These results are in complete agreement with previous structural data from LSDA calculations on similar systems.[9,27]

In the systems calculated with the HF method (Figure 3), we observe the reversal of carbon−carbon bond length alternation along the polyene segment contained between the Al bonding sites; that is, the initially double bonds in this segment of the molecule now show a single-bond character, and vice versa. In contrast, at the LSDA level of calculation (Figure 4), the lengths of the inner five carbon−carbon bonds are all typical of single bonds (∼1.44−1.45 Å), except for the central bond (∼1.41 Å) in the complex where the Al atoms are present on the same side of the polyene plane (bottom of Figure 4). This completely disrupts the π-conjugation and leads to loss of planarity for the organic molecule (∼15°), which is a clear indication of the sp^3 rehybridization of the carbon atoms. That the central bond maintains partial C═C character when the Al atoms are on the same side of the polyene plane is related to the fact that these Al atoms then interact to form an Al−Al bond of 2.60 Å; this results in only two Al−C bonds per Al, while Al atoms placed on opposite sides of the polyene plane form three Al−C bonds per Al. The experimental bond length in the aluminum dimer is reported to be 2.70 or 2.47 Å,[34] depending on the ground-state configuration, $^3\Pi_u$ or $^3\Sigma_g^-$, respectively. The formation of an Al−Al bond stabilizes the ground-state energy of the "same side" configuration by some 15 kcal/mol, compared to the other isomer of the complex; note that the same total energy difference obtained at the HF level is close to zero, a feature consistent with single Al−C bond formation.

The geometric differences between the HF and LSDA conformations prompted us to perform MP2 geometry optimizations on each complex. The resulting "same side" and "opposite

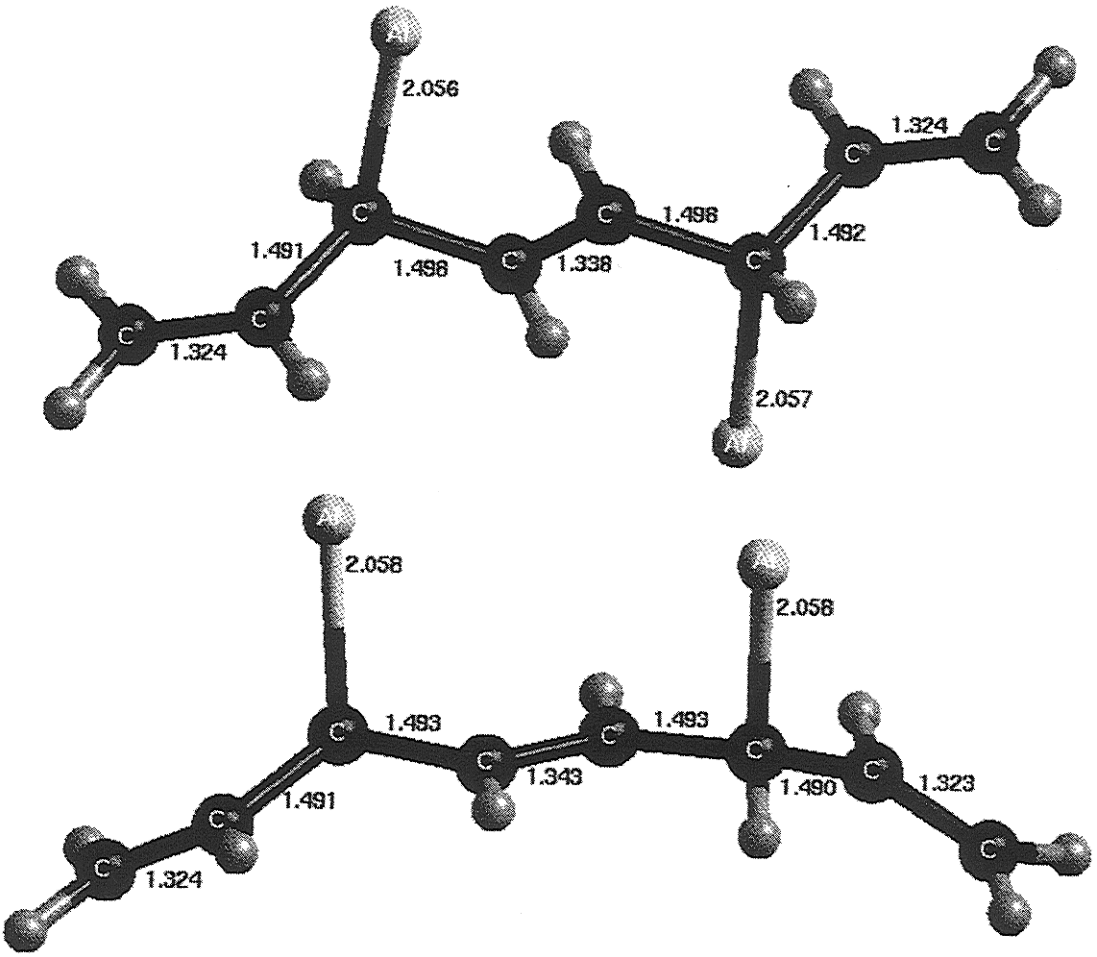

Figure 3. Chemical structures of Al_2/C_8H_{10} complexes, obtained at the HF level.

TABLE 5 : Changes in Mulliken and NPA (Presented in Brackets) Partial Atomic Charges (in $|e|$) in the Al_2/C_8H_{10} Complexes, Resulting from the Interaction Between Aluminum Atoms and the Polyene Molecule; See Table 3 for Labeling; The Bold Values Are Relative to the Atoms Involved in the Aluminum Bonding

	"same side" configuration		"opposite side" configuration	
	HF	LSDA	HF	LSDA
C1	−0.018 [−0.066]	−0.008 [−0.043]	−0.019 [−0.063]	−0.015 [−0.055]
C2	+0.048 [+0.039]	+0.026 [+0.012]	+0.047 [+0.040]	+0.039 [+0.018]
C3	**−0.339 [−0.730]**	**−0.149 [−0.429]**	**−0.346 [−0.726]**	**−0.158 [−0.449]**
C4	−0.010 [−0.050]	**−0.092 [−0.221]**	−0.009 [−0.046]	**−0.145 [−0.383]**
C5	+0.003 [−0.045]	**−0.097 [−0.224]**	+0.003 [−0.045]	**−0.142 [−0.384]**
C6	**−0.340 [−0.735]**	**−0.150 [−0.427]**	**−0.350 [−0.728]**	**−0.159 [−0.446]**
C7	+0.048 [+0.035]	+0.026 [+0.011]	+0.042 [+0.039]	+0.041 [+0.016]
C8	−0.019 [−0.065]	−0.007 [−0.040]	−0.017 [−0.064]	−0.014 [−0.052]
Al	**+0.358 [+0.799]**	**+0.130 [+0.589]**	**+0.374 [+0.782]**	**+0.216 [+0.806]**
Al	**+0.361 [+0.807]**	**+0.130 [+0.588]**	**+0.382 [+0.784]**	**+0.216 [+0.806]**

side" geometries are presented in Figure 5. It is important to note that for a given configuration ("same side" or "opposite side"), the optimized complex is the same, independently from starting from either the HF or the LSDA geometry. The resulting conformations are nearly identical to those resulting from the LSDA optimization, with the formation of multiple bonding between the aluminum atoms and the organic molecule and a similar reorganization of the π-conjugated system; the MP2 bond lengths are very close to those calculated at the LSDA level. Moreover, when starting the HF geometry optimization from the MP2-optimized configuration, the system comes back to its original HF configuration; equilibrium geometries are therefore markedly different according to the methodology used. These results thus stress the importance of taking explicitly into account electronic correlation to determine the structure of organometallic compounds; moreover, they illustrate that LSDA geometries are reliable and can be used with confidence to determine the vibrational frequencies of our systems.

Electronic Properties. Despite those geometric differences, the electronic properties calculated with HF and DFT are similar. When the two Al atoms bind to opposite sides of the molecule, the dipole moment of the complex remains close to zero, as expected for a quasi centrosymmetric arrangement. In contrast, the "same side" configurations possess a dipole moment of about 0.6 D, oriented parallel to the Al−C bonds, *i.e.* roughly perpendicular to the initial molecular plane.

Both population analyses (reported in Table 5) show the same tendencies, namely, a charge transfer from the Al atoms toward the oligomer. Note that NPA always provides larger values for the charge transfer relative to Mulliken analysis. This transfer leads to an increase in the electronic density of the

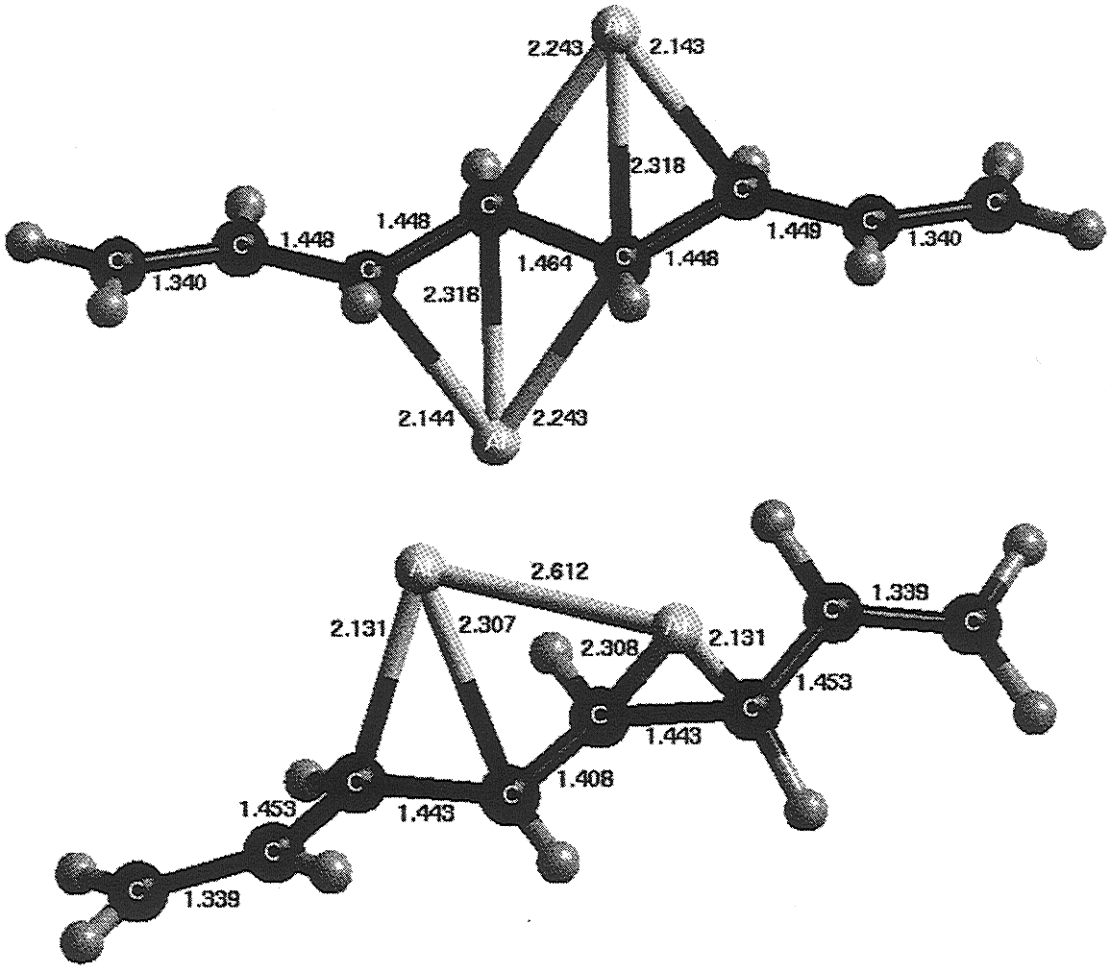

Figure 4. Chemical structures of Al_2/C_8H_{10} complexes, obtained at the LSDA level.

carbon atoms to which the metal atoms are bound. Accordingly, the electronic population of the four central carbon atoms is increased in the LSDA data, while in the HF configuration, only two carbon atoms become strongly negatively charged.

The description of the molecular orbitals in terms of linear combinations of atomic orbitals (LCAO) is very similar in the two theoretical approaches. Aluminum bonding corresponds to the hybridization of the Al_{3s} and Al_{3p} atomic orbitals with the π-molecular orbitals of the polyene. In particular, the HOMO (highest occupied molecular orbital) of the complexes is built from the combination of the LUMO (lowest unoccupied molecular orbital) of the pristine molecule and the valence levels of the metal atoms, which is consistent with the direction of charge transfer. The LCAO analysis of the upper electron levels of the complexes also shows that π-delocalization along the molecule is severely reduced.

Vibrational Properties. As we are interested in the spectral modifications following the interaction with aluminum, we have undertaken the vibrational analysis of the Al_2/C_8H_{10} complexes shown in Figures 3 and 4 (in this way, we can pinpoint the differences in the spectra related to multiple vs single Al−C bonding). The corresponding vibrational spectra are presented in Figure 6. The most striking observation on these spectra is the considerable increase in the number of peaks, compared to the pristine molecule. This comes from the loss of symmetry of the system; as a consequence, the analysis of the spectra becomes more difficult. In all four complexes, a very intense peak appears slightly below 1700 cm^{-1}. This mode originates from the stretching of the terminal C═C bonds, which have become isolated due to the loss of π-conjugation in the central part of the polyene. Charge transfer from the bonded Al atoms, contributing to an increase in molecular dipole moment, as well as the loss of planarity, can be responsible for the strong activity of this mode. It is also worth noticing that when the Al atoms are bonded on opposite sides of the polyene plane, the intensity of the 1700 cm^{-1} mode is significantly higher than when Al atoms are bonded to the same side of the molecule.

A second feature common to all spectra consists in the signature of the Al−C bonds: new bands appear in the region below 500 cm^{-1}, where pristine octatetraene is almost transparent (see Figure 2). For the LSDA structures, the two strongest Al−C stretching modes are located at 393 and 428 cm^{-1} for Al bonded to opposite sides and 348 and 418 cm^{-1} for Al bonded to the same side of the polyene plane. It is also important to mention the presence of another peak of significant intensity at 482 cm^{-1} in the spectra of the latter structure. This mode mainly corresponds to a vibration of the central C_2H_2 group. For the HF complexes, we also observe a new set of peaks below 500 cm^{-1}. In the opposite side configuration, the most important feature is the strong peak at 274 cm^{-1}. This mode involves the Al atoms and the central C_2H_2 group. Four peaks also appear below 500 cm^{-1}: at 348, 474, 478, and 499 cm^{-1}. The first one is related to a vibration of the entire molecule, while the other three are mostly Al−C stretching modes. In the same side configuration, we observe a similar behavior, the strongest intensity being this time located at 486 cm^{-1} and corresponding to an Al−C bond stretch. The mode at 445 cm^{-1} is also related to an Al−C stretch vibration, while the peak at 235 cm^{-1} involves only the C_2H_2 central group and

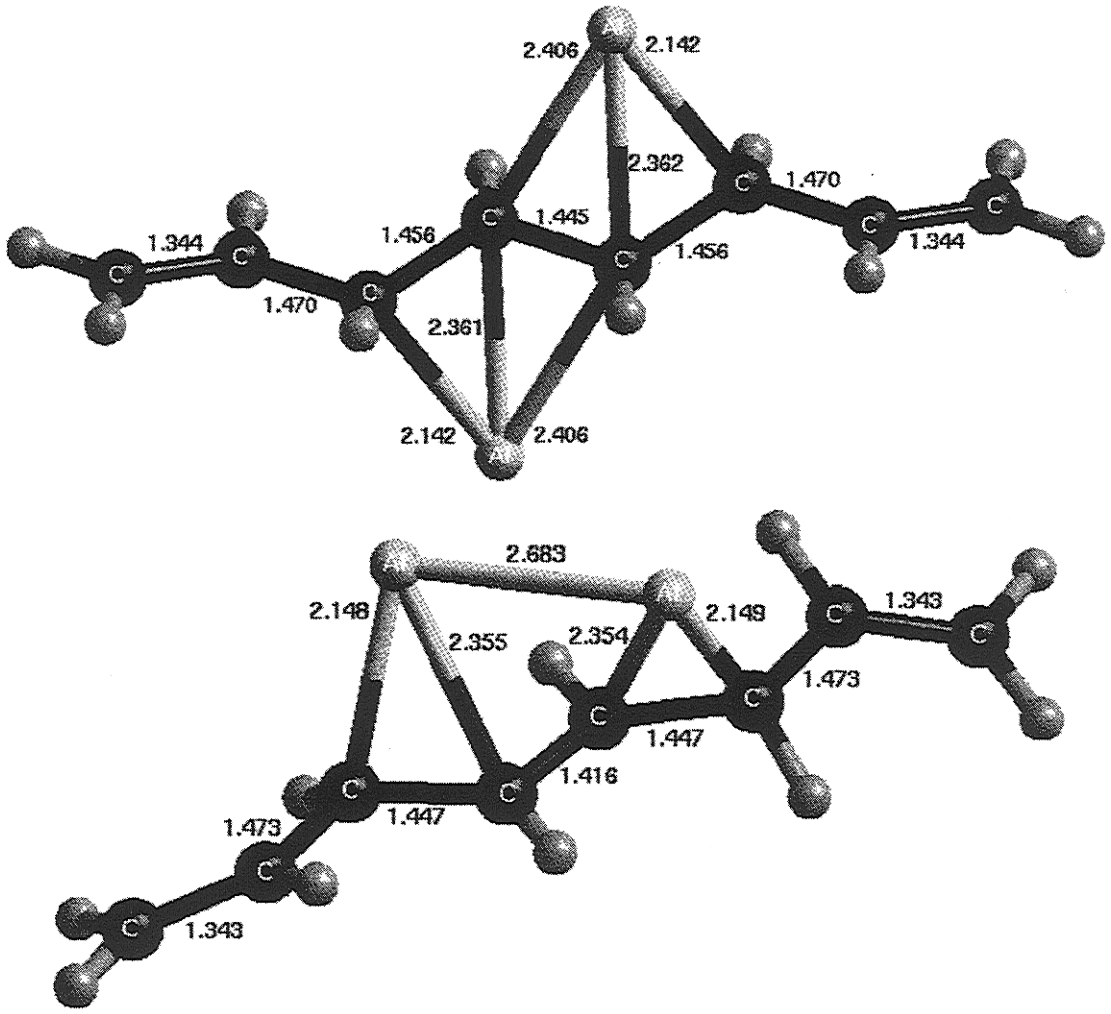

Figure 5. Chemical structures of Al_2/C_8H_{10} complexes, obtained at the MP2 level.

that at 290 cm^{-1} corresponds to the vibration of the entire molecule with both aluminum atoms. This part of the spectrum (0−500 cm^{-1}) is of considerable importance in the framework of this work for several reasons. First, it corresponds to the region where the modes involving the aluminum atoms are located. The appearance of new bands in this region of the experimental spectrum would thus confirm the existence of strong, covalent interactions between the polyene compound and aluminum. Moreover, the detailed analysis of this area could also allow one to asses how well the LSDA method performs.

In the 500−1500 cm^{-1} region, the major aspect of the HF results is the large number of modes appearing around 1000 cm^{-1}, which are not matched in the LSDA spectrum. This frequency region is mostly populated by modes involving bending of the hydrogen atoms, together with a carbon−carbon stretch component for those located at 1045 and 1084 cm^{-1} for the opposite side configuration, and those at 1038, 1050, and 1086 cm^{-1} for the same side configuration. An interesting aspect is that complexation leads to the appearance of peaks in previously transparent regions: for the complex where aluminum atoms are placed on opposite sides of octatetraene, new peaks occur at 506, 655, and 1420 cm^{-1}; for the other configuration, they are located at 656, 785, 1417, and 1421 cm^{-1}. Note that the modes around 1420 cm^{-1} in the complexes are similar to the modes located at 1405 cm^{-1} in the polyene molecule, that is, they essentially correspond to bending of the terminal hydrogens.

In the 500−1500 cm^{-1} region of the LSDA spectrum, the new structures can be identified by peaks at 752 and 778 cm^{-1}, in a region of the pristine molecule (700−800 cm^{-1}) devoid of vibrations. Those modes correspond to C−H bending vibrations involving the carbon atoms directly linked to the aluminum atoms. The relative weakness of the peaks around 1000 cm^{-1} could be a signature of structures consistent with LSDA (rather than HF) results, along with the intensity increase of the peaks just below 1200 cm^{-1}. Those modes include stretching components of the carbon−carbon single bonds that appear upon complexation. A signature of the opposite side LSDA configuration comes from the area below 1500 cm^{-1}, where two peaks stand at 1347 and 1436 cm^{-1}, while in the pristine system, only one peak of weaker intensity is situated at 1400 cm^{-1}. Those new modes correspond to the stretching of the carbon−carbon bonds of the backbone. Note that those vibrations are very weak in the IR spectrum of the configuration where the two aluminum atoms bind to the same side of the molecule.

Above 1500 cm^{-1}, the nature of the modes observed in the complexes is fundamentally different from the two modes calculated for the isolated C_8H_{10} molecule. The latter are replaced by the very intense peak described above (around 1680 cm^{-1}). We also observe a small peak just below this intense band in the HF spectrum of the C_8H_{10}/Al_2 complex with the aluminums on the same side. This satellite corresponds to the stretching of the central carbon−carbon bond, which has acquired a double-bond character following the complexation. This vibration is also observed in the opposite side configuration but with too weak an intensity to appear clearly in the spectrum. With the LSDA method, the change in single- and double-bond character is not as large as with the HF method, and no carbon−

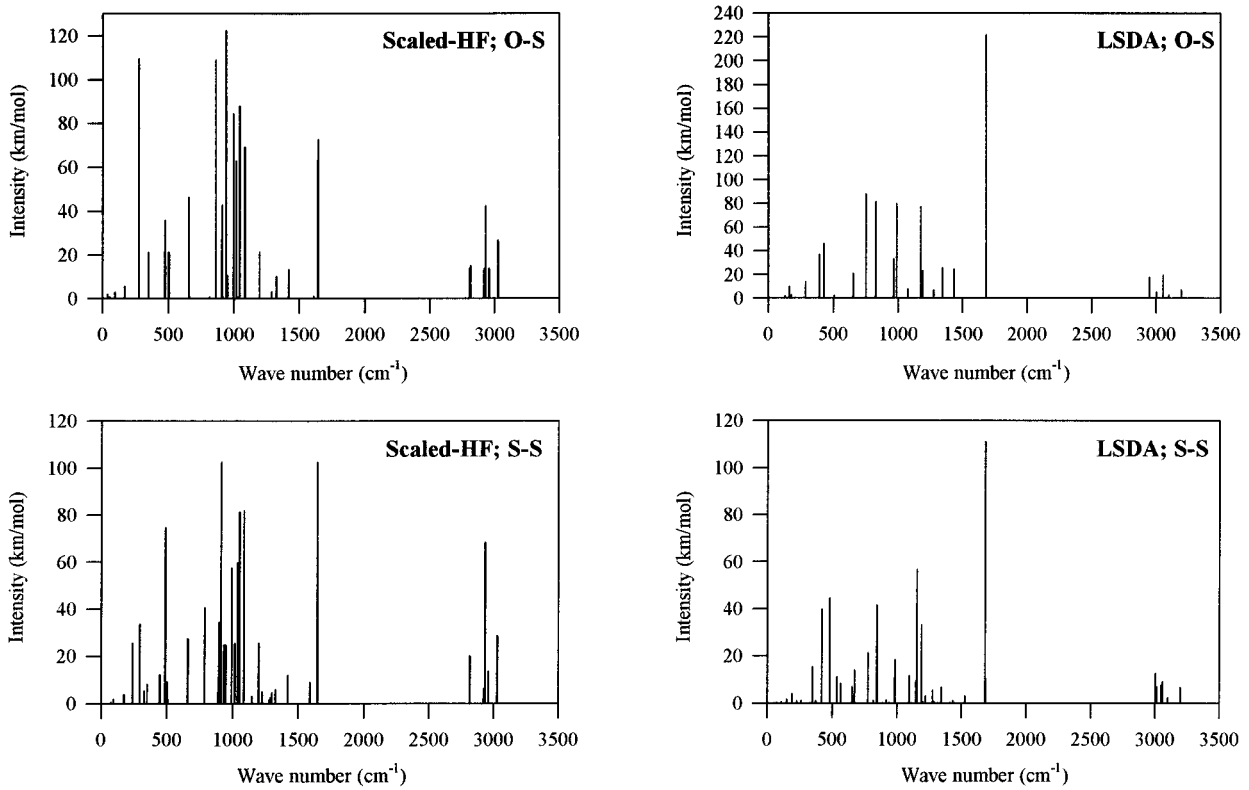

Figure 6. Calculated infrared spectra of Al_2/C_8H_{10} complexes: (left) HF spectra; (right) LSDA spectra; (top) opposite sides (O-S) configurations; (bottom) same side (S-S) configurations. Note that HF calculations on C_8H_{10}/Al_2 complexes give one small negative frequency (around -10 cm^{-1}). This means generally that the resulting conformation does not correspond to the global minimum but rather to a saddle point on the potential energy surface. In some cases, this can also originate from a spurious mixing of the low-frequency modes.[30] Nevertheless, we believe that this artifact does not influence significantly the frequencies that are of interest for vibrational analysis and comparison to experiment, *i.e.*, those above 100 cm^{-1}.

carbon double bond is left in the central part of the molecule, hence the lack of this mode. We also mention the very weak peak at 1529 cm^{-1} (same side LSDA configuration), corresponding to a simultaneous stretching of the three central carbon−carbon bonds involved in the interaction with aluminum.

Finally, upon complexation, the band around 3000 cm^{-1} containing the C−H stretching vibrations is broadened in both HF and LSDA calculations. The main difference between the two techniques is to be found in the intensity of that band, which is globally weaker with LSDA than with HF. Note also that the relative intensity decreases compared to the pristine molecule.

4. Synopsis

In the first part of this study, we have examined the reliability of HF and LSDA methods to calculate the vibrational spectra of polyenes. On the basis of theoretical and experimental data recently published on *trans*-butadiene and *trans*-octatetraene (*i.e.*, two model systems of polyacetylene), the techniques used in this work appear suitable for the intended study. The use of nonlocal functionals does not appear to be necessary for both geometry optimization and evaluation of the vibrational frequencies. Upon interaction of the polyene compound with two Al atoms, both the HF and LSDA techniques indicate the formation of Al−C covalent bonds. The results differ in that LSDA provides Al−C multiple bonding, while HF leads to Al−C single bonding. The LSDA octatetraene/aluminum geometries are found to be very similar to those from MP2 calculations; this shows the importance of electron correlation in the analysis of the interaction between metals and organic systems.

We find that the electronic properties (dipole moment, electron density distribution, description of the molecular orbitals) calculated with the HF and DFT techniques are very similar. Partial charge transfer occurs from the aluminum atoms toward the carbon atoms to which they are bound, thus increasing the electronic population on those atoms. The molecular orbitals are also deeply affected by the interaction. The highest occupied MOs are a combination between valence levels of the Al atoms and the π levels of the polyene molecule; their delocalized character is reduced.

We have determined the vibrational characteristics for Al/polyene complexes calculated by the *ab initio* HF and LSDA methods. In all cases, the strong interaction between aluminum and the polyene molecule leads to major changes in the spectra. The 0−500 cm^{-1} region can be used to establish a fingerprint for covalent Al−C bonding. Modes involving motions of the aluminum atoms (including Al−C stretching) lie in this region, at different frequencies and with different intensities depending on the multiple (LSDA) vs single (HF) bonding configuration of the metal atoms to the molecule. High vibrational intensity near 500 cm^{-1} would indicate the presence of Al atoms bonded to the same side of the polyene plane. Another interesting point is the appearance of new peaks in transparent areas of the pristine polyene molecule, *i.e.*, in the 700−800 cm^{-1} and 1300−1500 cm^{-1} regions.

We hope that the calculated modifications to the IR spectra described above will trigger future experimental work that could confirm the bonding pattern of aluminum to polyenes or polyacetylene. By comparison of the new bands appearing upon complexation in experimental and theoretical spectra, it should be possible to improve the understanding of the phenomena occurring at the interfaces between aluminum and π-conjugated systems.

Acknowledgment. The authors would like to thank Dr. D. Steel (McGill University, Montréal) and Dr. H. Verhoogt (Ecole Polytechnique de Montréal) for fruitful collaboration and many stimulating discussions. C.F. acknowledges funding from the Swedish National Research Council for Engineering Sciences (TFR). The work in Mons has been partly supported by the Belgian "Services Fédéraux des Affaires Scientifiques, Techniques et Culturelles (SSTC)" in the framework of the "Pôle d'Attraction Interuniversitaire: Chimie Supramoléculaire et Catalyse", FNRS/FRFC, and an IBM Academic Joint Study. The Mons−Montréal collaboration is supported by a Québec/Communauté Française de Belgique (CGRI) grant. V.P. is a FRIA grant holder.

References and Notes

(1) Burroughes, J. H.; Jones, C. A.; Friend, R. H. *Nature* **l988**, *335*, 137. Burn, P. L.; Holmes, A. B.; Kraft, A.; Bradley, D. D. C.; Brown, A. R.; Friend, R. H.; Gymer, R. W. *Nature* **1992**, *356*, 47.

(2) Braun, D.; Heeger, A. J. *Appl. Phys. Lett.* **1991**, *58*, 1982.

(3) Dannetun, P.; Lögdlund, M.; Fredriksson, C.; Boman, M.; Stafström, S.; Salaneck, W. R.; Kohler, B. E.; Spangler, C. in *Polymer-Solid Interfaces*; Pireaux, J. J., Bertrand, P., Brédas, J. L., Eds.; IoP: Bristol, 1992; p 201.

(4) Dannetun, P.; Lögdlund, M.; Fredriksson, C.; Lazzaroni, R.; Fauquet, C.; Stafström, S.; SpangIer, C. W.; Brédas, J. L.; Salaneck, W. R. *J. Chem. Phys.* **1994**, *100*, 6765.

(5) Dannetun, P.; Boman, M.; Stafström, S.; Salaneck, W. R.; Lazzaroni, R.; Fredriksson, C.; Brédas, J. L.; Zamboni, R.; Taliani, C. *J. Chem. Phys.* **1993**, *99*, 664.

(6) Boman, M.; Stafström, S.; Brédas, J. L. *J. Chem. Phys.* **1992**, *97*, 9144.

(7) Fredriksson, C.; Brédas, J. L. *J. Chem. Phys.* **1993**, *98*, 4253.

(8) Fredriksson, C.; Lazzaroni, R.; Brédas, J. L.; Dannetun, P.; Lögdlund, M.; Salaneck, W. R. *Synth. Met.* **1993**, *57*, 4632.

(9) Fredriksson, C.; Lazzaroni, R.; Brédas, J. L.; Ouhlal, A.; Selmani, A. *J. Chem. Phys.* **1994**, *100*, 9258.

(10) Fredriksson, C.; Lazzaroni, R.; Brédas, J. L.; Ouhla1, A.; Selmani, A. in *Metallized Plastics IV: Fundamental and Applied Aspects*; Mittal, K. L., Ed., in press.

(11) Parente, V.; Lazzaroni, R.; Selmani, A.; Brédas, J. L. *Synth. Met.* **1994**, *67*, 147. Parente, V.; Lazzaroni, R.; Brédas, J. L. To be published.

(12) Jones, R. O.; Gunnarson, O. *Rev. Mod. Phys.* **1990**, *61*, 689. *Density Functional Methods in Chemistry*; Labanowski, J., Andzelm, J., Eds.; Springer: New York, 1991. Ziegler, T. *Chem. Rev.* **1991**, *91*, 651.

(13) Lee, J. Y.; Hahn, O.; Lee, S. J.; Choi, H. S.; Shim, H.; Mhin, B. J.; Kim, K. S. *J. Phys. Chem.* **1995**, *99*, 1913.

(14) Lee, J. Y.; Hahn, O.; Lee, S. J.; Mhin, B. J.; Lee, M. S.; Kim, K. S. *J. Phys. Chem.* **1995**, *99*, 2262.

(15) Hirata, S.; Yoshida, H.; Torii, H.; Tasumi, M. *J. Chem. Phys.* **1995**, *103*, 8955.

(16) Frisch, M. J.; Trucks, G. W.; Schlegel, H. B.; Gill, P. M. W.; Johnson, B. G.; Wong, M. W.; Foresman, J. B.; Robb, M. A.; Head-Gordon, M.; Replogle, E. S.; Gomperts, R.; Andres, J. L.; Raghavachari, K.; Binkley, J. S.; Gonzalez, C.; Martin, R. L.; Fox, D. J.; Defrees, D. J.; Baker, J.; Stewart, J. J. P.; Pople, J. A. *Gaussian 92/DFT*; Gaussian, Inc.: Pittsburgh, PA, 1993.

(17) Hehre, W. H.; Ditchfeld, R.; Pople, J. A. *J. Chem. Phys.* **1972**, *56*, 2257. Hariharan, P. C.; Pople, J. A. *Theor. Chim. Acta* **1973**, *28*, 213. Gordon, M. S. *Chem. Phys. Lett.* **1980**, *76*, 163.

(18) Delley, B. *J. Phys. Chem.* **1990**, *92*, 508; **1991**, *94*, 7245.

(19) Vosko, S. H.; Wilk, L.; Nusair, M. *Can. J. Phys.* **1980**, *58*, 1200.

(20) Becke, A. D. *Phys. Rev. A* **1988**, *38*, 3098.

(21) Lee, C.; Yang, W.; Parr, R. G. *Phys. Rev. B* **1988**, *37*, 785.

(22) Perdew, J. P. *Phys. Rev. B* **1986**, *33*, 8822.

(23) Perdew, J. P.; Wang, Y. *Phys. Rev. B* **1992**, *45*, 13244.

(24) Wilson, E. B., Jr.; Decius, J. C.; Cross, P. C. *Molecular Vibrations*; Dover Publications, Inc.: New York, 1980.

(25) Wiberg, K. B.; Rosenberg, R. E. *J. Am. Chem. Soc.* **1990**, *112*, 1509.

(26) Miller, M. D.; Jensen, F.; Chapman, O. L.; Houk, K. N. *J. Phys. Chem.* **1989**, *93*, 4495.

(27) Fredriksson, C.; Stafström, S. *J. Chem. Phys.* **1994**, *101*, 9137.

(28) Mulliken, R. S. *J. Chem. Phys.* **1955**, *20*, 513.

(29) Glendening, E. D.; Reed, A. E.; Carpenter, J. E.; Weinhold, F. *NBO Version 3.1*.

(30) Del Zoppo, M. Private communication.

(31) Bock, C. W.; Panchenko, Y. N. *J. Mol. Struct.* **1989**, *187*, 69.

(32) Compton, D. A. C.; George, W. O.; Maddams, W. F. *J. Chem. Soc. Perkins Trans. 2* **1976**, 1666.

(33) Almenningen, A.; Halvorsen, S.; Haaland, A. *Acta Chem. Scand.* **1971**, *25*, 1937.

(34) Jones, O. *J. Chem. Phys.* **1993**, *99*, 1194.